

# OPTIMISING MECHANICAL PROPERTIES OF EPOXY MATRIX HYBRID COMPOSITES THROUGH SiC FILLER INTEGRATION AND FIBER REINFORCEMENT: THE TAGUCHI APPROACH

MURTHY ARUL,\* CHINNASAMY SUBRAMANIYAN,\*\* ERUSAGOUNDER SAKTHIVELMURUGAN\*\* and MYILSAM Y SURESHKUMAR\*\*

\**Department of Mechanical Engineering, ARM College of Engineering and Technology, Chennai 603209, India*

\*\**Department of Mechanical Engineering, Bannari Amman Institute of Technology, Sathyamangalam, Erode, 638401, Tamil Nadu, India*

✉ *Corresponding author: M. Arul, aruldevan1811@gmail.com*

*Received March 24, 2024*

This research aimed to enhance the mechanical properties of epoxy hybrid composites by reinforcing the plain-woven carbon fabric with the addition of SiC filler. The effects of varying SiC filler weights (5, 10 and 15 wt%), SiC filler sizes (26, 54 and 72  $\mu\text{m}$ ), and fiber orientations ( $0^\circ/90^\circ$ ,  $30^\circ/60^\circ$ , and  $45^\circ/45^\circ$ ) in hybrid epoxy composites on their mechanical properties were explored. A hand layup method was employed to fabricate the epoxy hybrid composites. Then, the fabricated samples were subjected to mechanical testing as per the ASTM standards. The inclusion of SiC particles led to a significant improvement in the performance of the epoxy hybrid composites. Moreover, the orientations of the fibers played a pivotal role in shaping the composite characteristics. Furthermore, Taguchi's  $L_9$  technique was used to identify the significant process parameters, resulting in a noteworthy 52% enhancement in efficiency compared to a full factorial design. Also, this study showed cost-effectiveness and resource efficiency by employing the Taguchi  $L_9$  technique over the full factorial design. Finally, the study concluded that significant parameters, including SiC particle size of 26  $\mu\text{m}$ , fiber orientation of  $0^\circ/90^\circ$ , and particle weight ranging from 10 to 15%, enhanced the mechanical performance of the composites.

**Keywords:** epoxy hybrid composite, plain-woven carbon fabric, SiC filler, fiber orientation, mechanical properties, Taguchi  $L_9$  technique

## INTRODUCTION

Over the past two decades, polymer composites have gained significant popularity as a viable alternative to traditional materials in various applications that demand high strength and lightweight characteristics. This surge in popularity can be attributed to their exceptional toughness, thermal stability, and favourable strength-to-weight ratio. The performance of these composites is influenced by a combination of factors, such as the characteristics of the fillers, their shape, matrix properties, interactions between fillers and the matrix, filler alignment within the matrix, and the volume percentage of fillers.<sup>1</sup> Among thermosetting polymers, epoxy resin has emerged as a preferred choice in engineering applications due to its numerous advantageous properties.<sup>2,3,4</sup> Notable features of

epoxy resin include low shrinkage, enhanced rigidity, high resistance to chemicals and corrosion, excellent adhesive capabilities, favourable thermomechanical properties, and commendable dielectric strength. Moreover, epoxy resin exhibits remarkable compatibility with a vast range of materials, such as metals, glass, plastics, ceramics, stone, and wood.<sup>5</sup>

In recent decades, researchers have extensively investigated the potential of reinforcing epoxy resin with natural fibers, synthetic fibers, and other reinforcement particles.<sup>6</sup> Synthetic fiber-reinforced epoxy composites, renowned for their lightweight nature, high strength, and superior modulus, find widespread applications in the automotive and construction industries.<sup>7,8,9</sup> A sheet of carbon fiber with a plain weave features a

refined, symmetrical checkerboard pattern. In this particular weave, the tows are arranged using an over/under pattern, resulting in a distinct interlacing structure. The close spacing of these interlaced tows contributes to the plain weave's exceptional stability and robustness.<sup>10,11</sup> Due to its tighter weave, which makes it easier to handle without distorting them. The physical and geometric characteristics strongly influence the mechanical behaviour of epoxy matrix composites added with fibers, in addition to the chemical composition of the fiber.<sup>12</sup>

Woven fabrics have greater strength and structural integrity compared to non-woven fabrics.<sup>13-16</sup> The number of fabric layers also influences the composite strength. In a study, Md. Abu ShaidSujon *et al.* investigated the effects of four distinct stacking sequences and three fiber orientations. According to their experimental research, the stacking order significantly affects the flexural property, whereas the fiber orientation has an impact on the tensile property. Additionally, it was discovered that the impact strength is not noticeably affected by the stacking order.<sup>17</sup> Nurain Hashim *et al.* examined the performance of a woven interplay of a hybrid composite consisting of carbon and kevlar reinforcement in an epoxy matrix under both static and cyclic loading conditions.<sup>18</sup> The characteristics of the fibers that are aligned with the loading direction were shown to be substantially correlated with tensile properties and fatigue behaviour. Invoking hybridization in the composites improved performance and efficiency.

To address the limitations of polymer composites, synthetic fillers have been added to enhance material properties and reinforce the fiber-matrix interface. Muralidhara *et al.* conducted a study examining the tribological, thermal and mechanical characteristics of composites with epoxy matrix reinforced by carbon fibers with the addition of BN particles. The study revealed significant enhancements in tribological, mechanical and thermal properties due to the inclusion of BN-CF/Ep composites.<sup>19</sup> Alsaadi investigated the enhanced flexural behaviour of composites reinforced with carbon and aramid fibers containing silicon carbide (SiC) particles. The study also focused on the interlaminar fracture behaviour related to mode-II delamination.<sup>20</sup> The findings demonstrated that aramid fiber-reinforced epoxy-SiC composites exhibit improved delamination and flexural

properties than carbon fiber-reinforced epoxy-SiC composites. Cho *et al.* conducted a study exploring the mechanical properties of polymer hybrid composites, particularly those with spherical particles, which will be significantly influenced by the incorporation of particles with different shapes and sizes.<sup>21</sup> Reducing particle sizes can improve the tensile behaviour of composites. Experimental observation and numerical analysis indicated minimal influence due to the size of the particle on the fracture toughness against the interfacial strength between particles and the matrix. Kumaresan *et al.* conducted a study investigating the improvement of friction and wear behaviour in the epoxy composite reinforced with carbon fabric by incorporating silicon carbide as a filler.<sup>22</sup> This approach aims to explore the potential structural applications of epoxy hybrid composites by reinforcing the plain-woven carbon fabric with SiC filler.

The Taguchi approach has been extensively applied across various fields, showcasing its versatility and effectiveness in optimization processes. Researchers have utilized Taguchi's robust experimental design to enhance outcomes in areas such as composite material development, machining processes, thermo-electric generation, and environmental remediation.<sup>23,24,25</sup> Under these circumstances, Taguchi's tool improves product performance, process efficiency, and overall quality through parameter optimization.<sup>26,27,28</sup>

From a thorough literature survey, it has been found that the researchers have developed a variety of epoxy hybrid composites for structural applications.<sup>29,30,31</sup> However, no one has attempted the fabrication of epoxy hybrid composites by reinforcing the plain-woven carbon fabric with the addition of SiC filler varying SiC particle size, SiC weight percentage, and fiber orientations simultaneously. Moreover, no attention has been given to the integration of the Taguchi L<sub>9</sub> approach with the ANOVA method for experimental design. In this context, optimization of design parameters, such as filler particle size, weight fraction, and fiber orientation, in epoxy hybrid composites remains unexplored. Therefore, this study aims to fill this gap by using the Taguchi method to enhance the fracture properties of plain-woven carbon fabric-reinforced epoxy composites with the addition of SiC filler. Also, the effect of varying SiC particle size, SiC weight percentage, and fiber orientations

on the mechanical properties of epoxy hybrid composites was examined.

## EXPERIMENTAL

### Materials

In this study, Araldite LY 556 was used as an epoxy matrix, with viscosity and density of 10-12 Ns/m<sup>2</sup> and 1.15-1.20 g/cm<sup>3</sup>, respectively. Additionally, Araldite HY 951 was employed as a hardener that is mixed with the epoxy resin in the ratio of 100:10. The hardener is a clear liquid, with a flash point of 110 °C and specific gravity of 0.98 g/cm<sup>3</sup> at 25 °C (supplied by Ciba Geigy India Ltd.). The filler material utilized was SiC particles, available in three different sizes: 26 µm, 54 µm, and 72 µm, with a 2.6 g/cm<sup>3</sup> density. Carbon fibers in a plain-woven fabric configuration were chosen as reinforcement fibers. The polymer

matrix hybrid composites consist of epoxy resin, carbon fibers (stacked in eight layers with a constant fabric weight fraction of 20 wt%), and varying filler contents (0, 5, 10, 15 and 20 wt%).

### Experimental design

To attain optimal product quality through design, Taguchi proposes a three-stage approach, which includes system design, tolerance and parameters. Taguchi's L<sub>9</sub> orthogonal array is used to identify the optimal combination of parameters, such as fiber orientation, filler material size, and weight percentage. The parameters and their levels are detailed in Table 1. Also, the experimental design strategy is shown in Figure 1.

Table 1  
Parameters and their levels

S.No	Parameters	Level 1	Level 2	Level 3
1	SiC filler (wt%)	5	10	15
2	SiC particle size (µm)	26	54	72
3	Fiber orientation (angle)	0°/90°	30°/60°	45°/45°

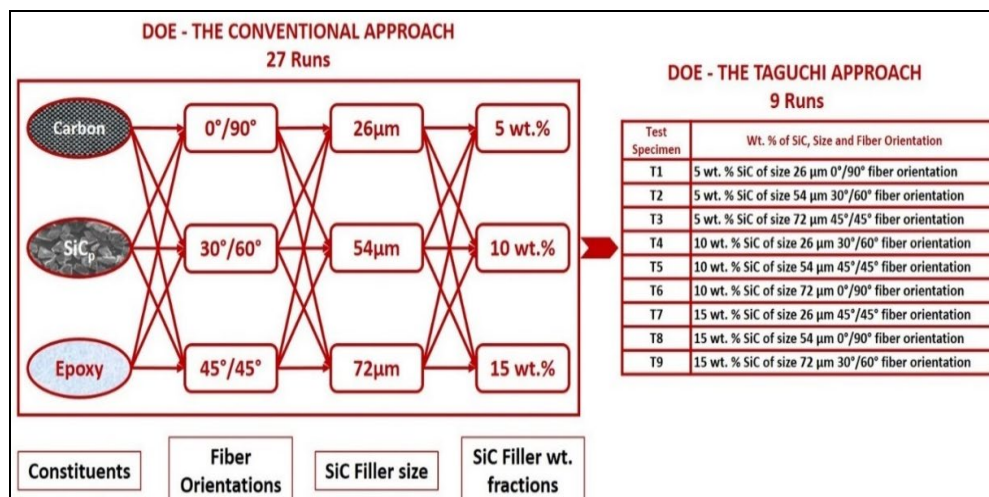


Figure 1: Taguchi L<sub>9</sub> experimental design strategy

### Processing method

The hand lay-up process is a well-established method used in the manufacturing of polymer matrix composites.<sup>32-34</sup> It requires several sequential steps to ensure that the desired properties and structural integrity are achieved. The process involves four main stages: mould preparation, gel coating, lay-up, and curing. The first step involves preparing the mould for the composite. This typically involves cleaning and applying release agents to ensure easy removal of the finished composite. The isophthalic gelcoat was used in this process; it acts as a protective barrier between the mold surface and gelcoat. It also helps to prevent

adhesion and facilitates smooth release without compromising the integrity of the gelcoat layer.

In the lay-up stage, composite materials, such as fiber mats and a resin matrix, are laid up onto the mould surface. In the process described here, epoxy resin mixed with SiC particles was applied to the fiber mat using a hand roller to ensure even distribution of the resin across the woven fabrics. Multiple layers were stacked together to achieve the desired thickness and properties. The stacking method used here includes orientations of 0°/90°, 30°/60°, and 45°/45° for improved strength and flexibility.

Once the lay-up was complete, the composite was subjected to curing. In the described process, epoxy

resin mixed with a hardener in a specific ratio was used. The curing process typically involves applying pressure to the composite and allowing it to cure for a specified period. This ensures proper bonding and consolidation of the composite materials. After the curing process, the composite specimen was removed from the mould and allowed to cure further if necessary. Samples were then extracted from the laminates according to ASTM standards for further testing.

The fabrication method of epoxy hybrid composites is shown in Figure 2. The tests included evaluating tensile properties, hardness, interlaminar strength, and flexural strength to assess the performance of the composite material. For optimization purposes, better characteristics were selected to maximize the output responses. The S/N ratio and percentage influence were calculated by using Equations (1) and (2):

$$S/N = -10 \log_{10} \frac{1}{n} \left[ \sum_{i=1}^n \frac{1}{y_i^2} \right] \quad (1)$$

where n = number of tests in a trial and  $y_i$  corresponding output values.

$$\text{Percentage of influence by parameter} = \frac{SS_{\text{Parameter}}}{SS_{\text{Total}}} \quad (2)$$

**Testing methods**

To analyze the structure of the prepared epoxy hybrid composites, a Rigaku Mini Flex II-C X-ray diffractometer, with CuK  $\alpha$  radiation ( $\lambda = 1.540 \text{ nm}$ ), was used. X-ray diffraction patterns were recorded at a scanning rate of  $1^\circ/\text{min}$ .

The Vickers microhardness test was carried out using the ASTM E92 standard.<sup>35,36</sup> The tensile behaviour of the composite was analyzed using a UTM machine (Instron 1195), following the ASTM 3039 standard.<sup>37,38</sup> The specimens used for tensile testing had a length of 200 mm, a width of 11.5 mm, and an equivalent thickness to the composite material composition. Interlaminar shear strength (ILSS) was determined using the ASTM D5528 standard, utilizing the UTM equipment.<sup>39,40</sup> The evaluation of flexural strength followed the guidelines outlined in the ASTM D790 standard.<sup>41,42</sup> The three-point method was used to assess the flexural strength of the specimens, with a length of 157 mm, a width of 12.7 mm, and a thickness corresponding to the composite composition. Prepared specimen samples are depicted in Figures 3 and 4, respectively.

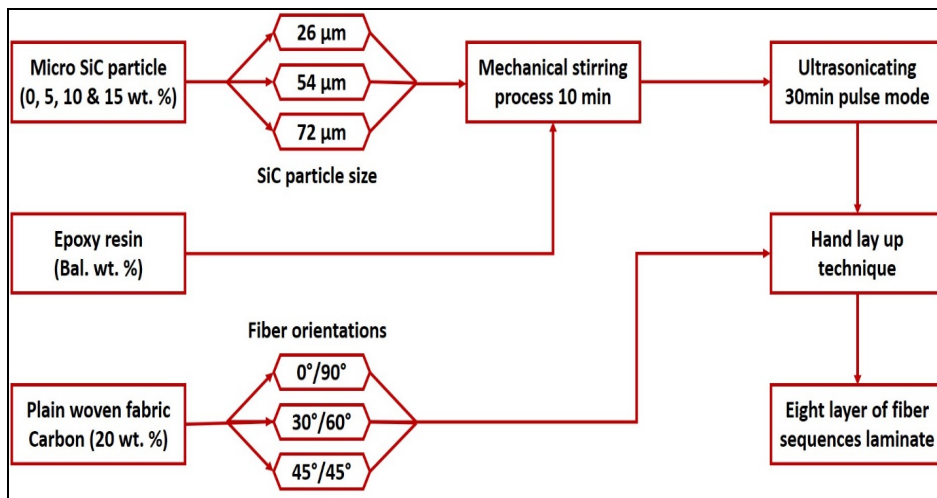


Figure 2: Fabrication method of epoxy hybrid composites

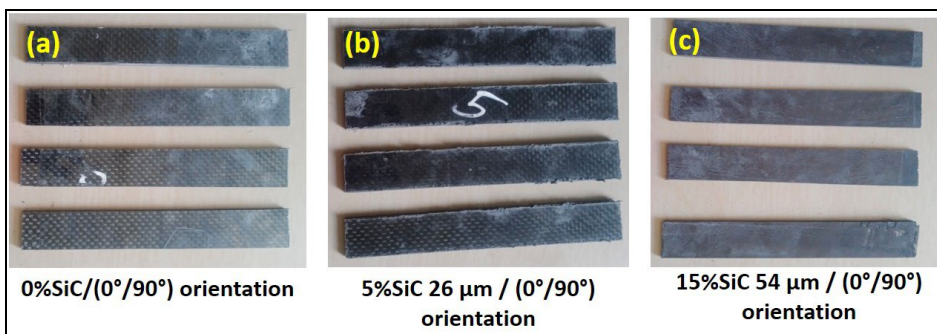


Figure 3: Flexural test specimens of epoxy hybrid composites

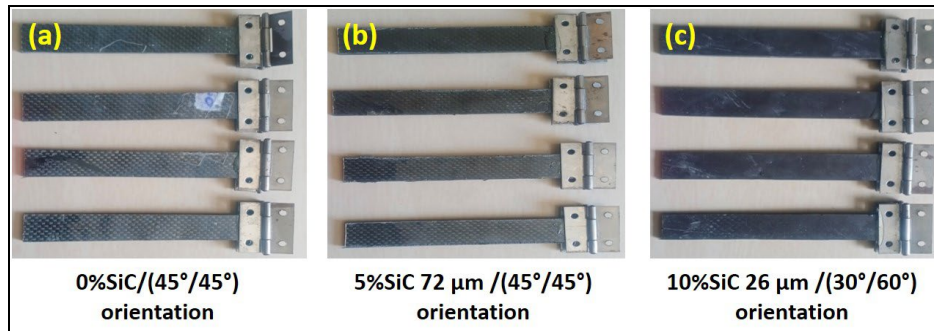


Figure 4: ILSS test specimens of epoxy hybrid composites

## RESULTS AND DISCUSSION

### XRD analysis

The XRD analysis of the epoxy hybrid composite (10% SiC/26  $\mu\text{m}$  SiC filler size/0°/90° fiber orientation) was conducted to investigate the material's crystalline structure and phase composition. This proportion was chosen based on the study's identification of optimal parameters to enhance composite performance. Specifically, the study found that using SiC particles with a size of 26  $\mu\text{m}$ , a fiber orientation of 0°/90°, and a particle weight percentage ranging from 10 to 15% significantly improved the composite's properties. Therefore, conducting XRD analysis on this specific composite proportion allows for a thorough understanding of its structural characteristics and validating its optimised parameters.

The XRD analysis conducted on the SiC-reinforced composite materials revealed a highly crystalline structure during the curing process, as shown in Figure 5. The (400), (311), (220), and (111) planes corresponding to the distinct peaks at 69.4, 56.3, 47.6, and 28.7°, respectively, were observed in the XRD patterns, for the arrangement of the eight-layer composite laminate

plate. Notably, no noticeable peaks indicative of various carbon and only the epoxy composite types were observed, suggesting that the materials possessed an amorphous nature.

### Studies on mechanical properties

The orientation of the fibers has a significant impact on the mechanical properties of laminated composites. The tensile performance of the laminates is mostly determined by the viscoelastic characteristics of the epoxy matrix and the strength of the interface. The three experimental design parameters are filler particle weight fractions (5%, 10%, and 15%), filler particle sizes (26  $\mu\text{m}$ , 54  $\mu\text{m}$ , and 72  $\mu\text{m}$ ), and fiber orientations (0°/90°, 30°/60° and 45°/45°). To estimate the impact of these three factors on the hardness, tensile, flexural, and ILSS of the composites, ANOVA analysis was performed using Minitab 16.0. This study has successfully determined the optimal values for the influential factors. Table 2 shows the hardness, flexural, tensile, and ILSS of carbon fiber-reinforced epoxy composites with various fiber orientations without SiC filler.

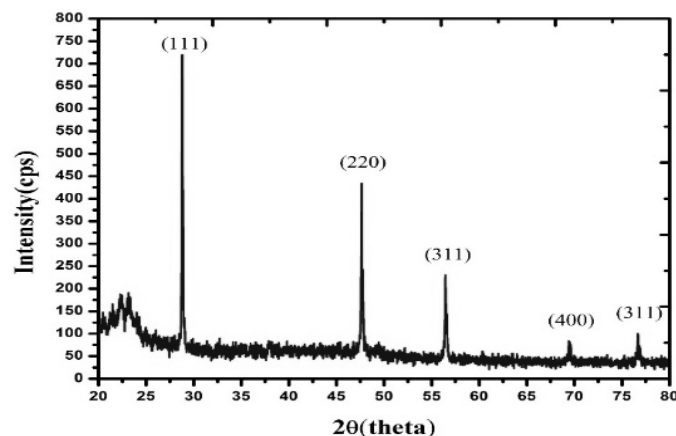


Figure 5: XRD plot for epoxy hybrid composite (10% SiC/26  $\mu\text{m}$ /0°/90°)



Table 2  
Mechanical test results of epoxy hybrid composites (without SiC filler)

S.No	Fiber orientation (angle)	Hardness (HV)	Tensile strength (MPa)	ILSS (MPa)	Flexural strength (MPa)
1.	(0°/90°)	132±4	231±5	170±4	94±2
2.	(30°/60°)	116±3	192±4	142±2	81±2
3.	(45°/45°)	107±3	129±4	109±3	65±2

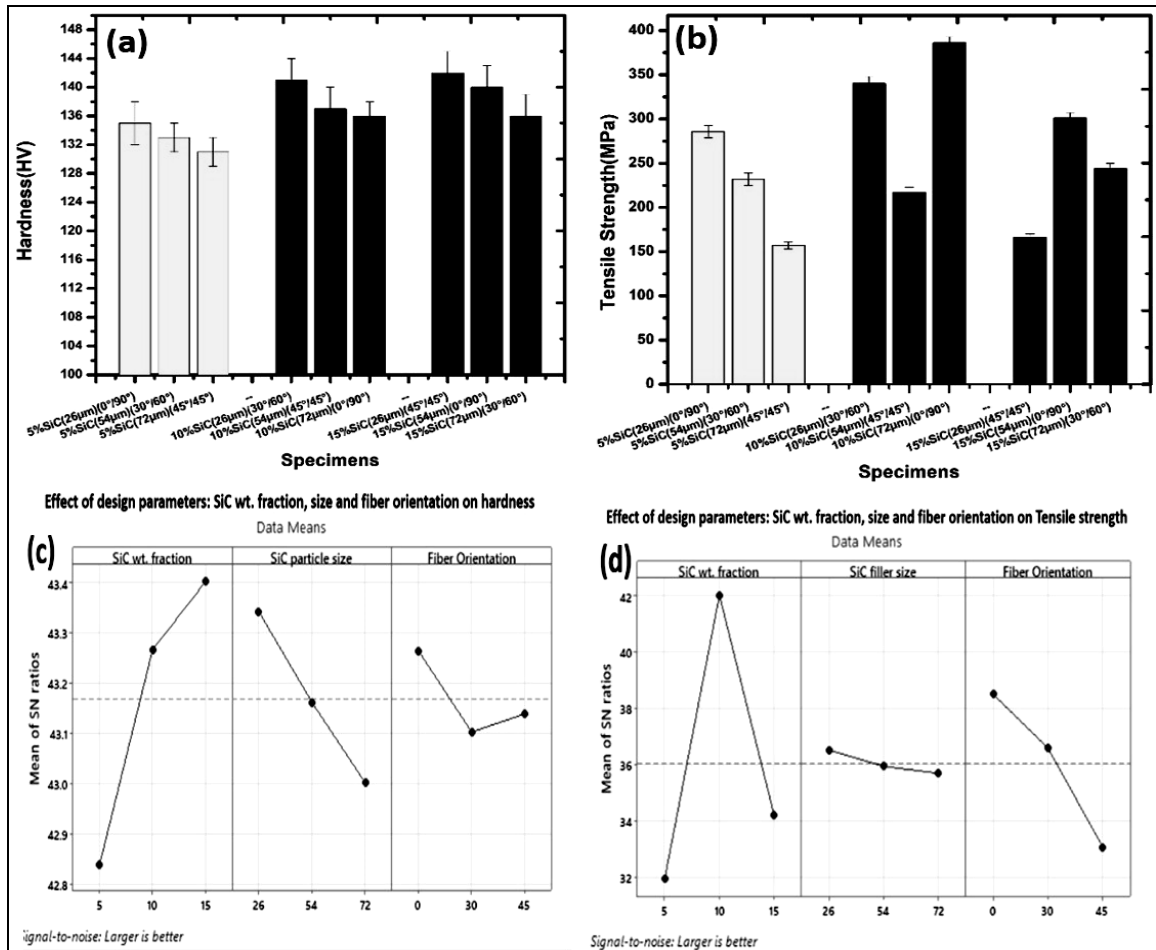


Figure 6: (a, b) ANOVA results of hardness and tensile test; (c, d) hardness and tensile test main effects plots for S/N ratios

**Hardness and tensile tests**

The performed experiments have clarified the key aspects that affect the mechanical performance of epoxy hybrid composites when reinforced with various fillers. These factors include the filler volume percentage, aspect ratio and orientation of fillers, and adhesion between the filler and matrix. The results indicate that, with an increasing composite density, attributed to the arrangement of fillers between the composite matrix and fibers, there is a corresponding increase in the hardness value. The experimental values of hardness (HV) and tensile strength

(MPa) are plotted in Figure 6 (a) and (b), respectively.

The investigation was conducted with a 95% confidence level to estimate the relative behaviour of the composites. Figure 6 (c) presents the hardness test main effects plot for S/N ratios, where the combination of a particle size of 26 μm, 15 wt% filler, and a 0°/90° fiber orientation showed statistical significance and achieved the highest predicted hardness value of 152.44.

The ANOVA analysis, as shown in Table 3, revealed that the filler particle weight fraction had the most significant impact on hardness (68.78%),

followed by filler size (23.17%) and fiber orientation (5.7%). Various factors affect the strength of composites reinforced with woven fibers, including weave design, the bonding between the matrix and fiber, *etc.* Notably, the plain weave pattern demonstrates higher tensile strength, as it facilitates uniform stress distribution during load application in both the axial and cross-sectional directions. The longitudinal orientation of stronger and stiffer fibers enables superior stress absorption and enhanced mechanical strength. For SiC-filled plain woven fabric carbon fiber-reinforced epoxy composites, the tensile strength exhibited an upward trend with an increase in SiC content up

to 10 wt%. However, when the filler weight fraction exceeded 10%, decreased tensile strength was observed in the agglomeration phenomenon of SiC particles and the formation of void content. Figure 6 (d) displays the tensile test main effects plot for S/N ratios, where the combination of a SiC particle size of 26  $\mu\text{m}$ , 10 weight percentage of filler, and  $0^\circ/90^\circ$  fiber orientation achieved the highest predicted tensile value of 385.11. According to the ANOVA analysis in Table 3, fiber orientation had the most important influence on tensile strength (73%), followed by filler particle weight fraction (26%) and filler size (1%).

Table 3  
ANOVA results for hardness and tensile test

Test	Source	DF	Seq. SS	Adj. SS	Adj. MS	F	P
Hardness	SiC wt. fraction	2	0.52102	0.52102	0.260512	29.59	0.033
	SiC particle size	2	0.17555	0.17555	0.087776	9.97	0.091
	Fiber orientation	2	0.04330	0.04330	0.021651	2.46	0.289
	Residual error	2	0.01761	0.01761	0.008803		
	Total	8	0.75748				
Tensile	SiC wt. fraction	2	14.7200	14.7200	7.3600	177.46	0.006
	SiC particle size	2	0.1029	0.1029	0.0515	1.24	0.446
	Fiber orientation	2	41.3597	41.3597	20.6799	498.61	0.002
	Residual error	2	0.0829	0.0829	0.0415		
	Total	8	56.2656				

### Flexural strength and ILSS

To examine the bending behaviour of composite materials, a three-point test for the flexural study was utilized. The bending strength of composites is typically influenced by both compressive and shear strength factors. Weaving patterns play a crucial role in creating an interlocking structure through the combined influence of warp and weft fiber threads.

This interlocking structure effectively restricts the extension of fiber yarns in both the transverse and longitudinal directions, leading to the enhanced load-carrying capacity of the fibers during bending.<sup>43</sup> The experimental results are illustrated graphically in Figure 7 (a) and (b), respectively, which show the plotted data for flexural strength (MPa) and ILSS (MPa). Figure 7 (c) illustrates flexural strength main effects plot for S/N ratios, where the combination of a SiC particle size of 26  $\mu\text{m}$ , 10 wt% filler, and  $0^\circ/90^\circ$  fiber orientation, which yielded the highest predicted flexural strength value of 112.11. The ANOVA analysis in Table 4 revealed that fiber

orientation had an important influence on flexural strength (86.56%), followed by filler size (10.1%) and filler particle weight fraction (2.87%).

Interlaminar fracture or delamination damage is a significant concern in composites laminated by fibers. The fracture behaviour of composites is influenced by various factors, including loading speed, stress concentration, temperature, and thermal shock. In woven-fabric composites, the non-planar interlaminar structure, combined with the interaction between delamination cracks, matrix regions, and weave structure, contributes to crack formation during crack propagation. The ASTM D5528 standard specimen and double cantilever beam (DCB) specimens are used to estimate the fracture toughness model-I of continuous fiber-reinforced composite materials. Figure 7 (d) shows interlaminar shear strength main effect plot for S/N ratios, where the combination of a SiC particle size of 26  $\mu\text{m}$ , 15 wt% filler, and a  $0^\circ/90^\circ$  fiber orientation resulting in the highest predicted ILSS value of 272.11. The ANOVA analysis in Table 4 indicated that

fiber orientation had the most significant impact on ILSS (75.20%), followed by filler particle

weight fraction (21.52%) and filler size (3%).

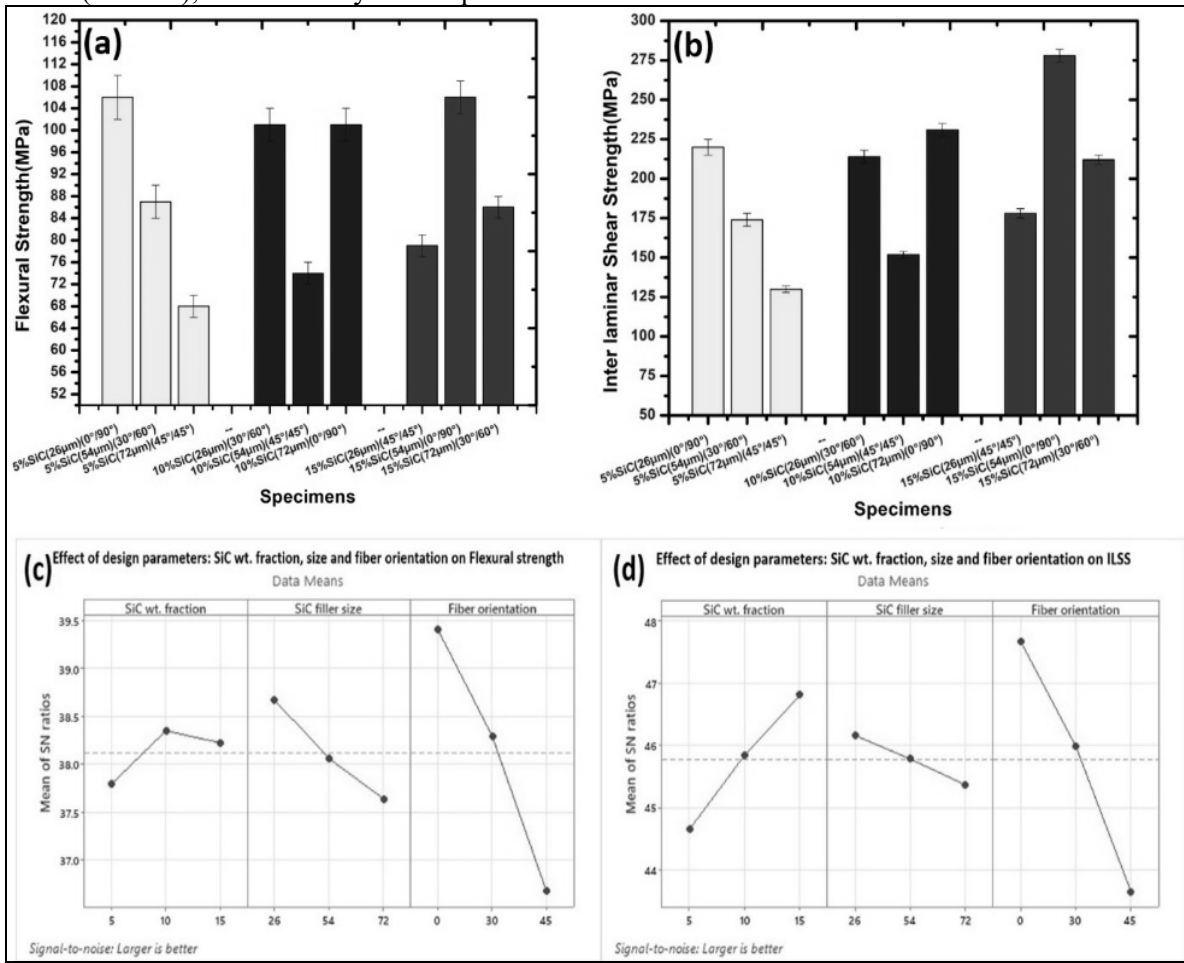


Figure 7: Epoxy hybrid composite (a) Flexural strength, (b) ILSS, (c, d) Flexural strength and ILSS main effects plots for S/N ratios

Table 4  
ANOVA results for flexural strength and ILSS

Test	Source	DF	Seq. SS	Adj. SS	Adj. MS	F	P
Flexural strength	SiC wt. fraction	2	0.4674	0.4674	0.23370	6.27	0.138
	SiC particle size	2	1.6415	1.6415	0.82074	22.02	0.043
	Fiber orientation	2	14.0689	14.0689	7.03445	188.72	0.005
	Residual error	2	0.0745	0.0745	0.03727		
	Total	8	16.2523				
ILSS	SiC wt. fraction	2	7.0192	7.0192	3.5096	61.01	0.016
	SiC particle size	2	0.9506	0.9506	0.4753	8.26	0.108
	Fiber orientation	2	24.5256	24.5256	12.2628	213.18	0.005
	Residual error	2	0.1150	0.1150	0.0575		
	Total	8	32.6104				

**Optimization of design parameters**

Based on the test results, it is evident that SiC filler size, SiC weight fraction and fiber orientation had a significant effect on the mechanical properties of the epoxy hybrid

composites. The following inferences have been made from the mechanical test results. The fiber orientation has a relatively low influence (5.7%), while filler size (23.17%) and weight fraction (68.78%) have a significant impact on hardness.



The fiber orientation has a high influence (73%) on tensile strength, while weight fraction (26%) and filler size (1%) have lower effects. Fiber orientation (86.56%) is the factor that enhances flexural strength, whereas filler size (10%) and weight fraction (2.89%) have comparatively minor impacts. Fiber orientation (75.20%) and weight fraction (21.52%) are the primary influencing factors on ILSS, while filler size (3%) has the least influence.

Based on the ANOVA results, the optimized fiber orientation and SiC filler particle size were determined to be  $0^{\circ}/90^{\circ}$  and  $26\ \mu\text{m}$ , respectively. Table 5 shows the ANOVA-predicted optimized design factors. Figure 8 provides an overview of the composites' hardness and tensile strength with various weight fractions of SiC, a particle size of  $26\ \mu\text{m}$ , and a  $0^{\circ}/90^{\circ}$  fiber orientation. As the SiC weight percentage increases in the composite,

there is a general trend of improving mechanical properties. Hardness values consistently rise from 132 HV (0% SiC) to 153 HV (20% SiC), indicating that incorporating SiC contributes to increased hardness. The higher density resulting from the filler particles between the matrix and fibers is responsible for this hardness improvement. Additionally, the tensile strength shows a positive correlation with increasing SiC content, reaching a peak at 10% SiC (231 to 378). However, beyond this point, the tensile strength decreases (301 for 15% SiC and 291 for 20% SiC). This reduction in strength can be attributed to SiC particles resisting load transfer and agglomeration, leading to weakened bonding strength. Figure 9 provides an overview of the composites' flexural strength and ILSS with various weight fractions of SiC, a particle size of  $26\ \mu\text{m}$ , and  $0^{\circ}/90^{\circ}$  fiber orientation.

Table 5  
ANOVA for predicted optimized design parameters

Test	Composite composition	ANOVA predicted result	Experimental values	Parameter influence
Hardness	$26\ \mu\text{m}/15\ \text{wt}\% \text{ SiC}$ with $0^{\circ}/90^{\circ}$ orientation	152.44	$152 \pm 13\ \text{HV}$	WF – 68.78% FS – 23.17% FO – 5.7%
Tensile	$26\ \mu\text{m}/10\ \text{wt}\% \text{ SiC}$ with $0^{\circ}/90^{\circ}$ orientation	385.11	$378 \pm 24\ \text{MPa}$	FO – 73% WF – 26% FS – 1%
Flexural strength	$26\ \mu\text{m}/10\ \text{wt}\% \text{ SiC}$ with $0^{\circ}/90^{\circ}$ orientation	112.11	$112 \pm 7\ \text{MPa}$	FO – 86.56% FS – 10.1% WF – 2.89%
ILSS	$26\ \mu\text{m}/15\ \text{wt}\% \text{ SiC}$ with $0^{\circ}/90^{\circ}$ orientation	272.111	$270 \pm 14\ \text{MPa}$	FO – 75.20% WF – 21.52% FS – 3%

FO – fiber orientation; FS – SiC filler size; WF – weight fraction of SiC

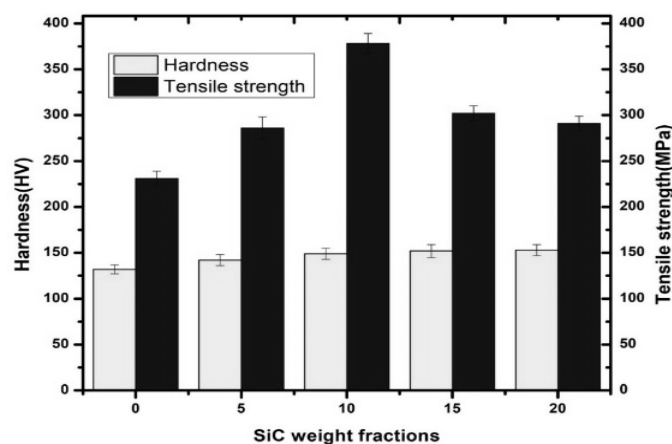


Figure 8: Hardness and tensile value of composites with various weight fractions of SiC/ $26\ \mu\text{m}/0^{\circ}/90^{\circ}$

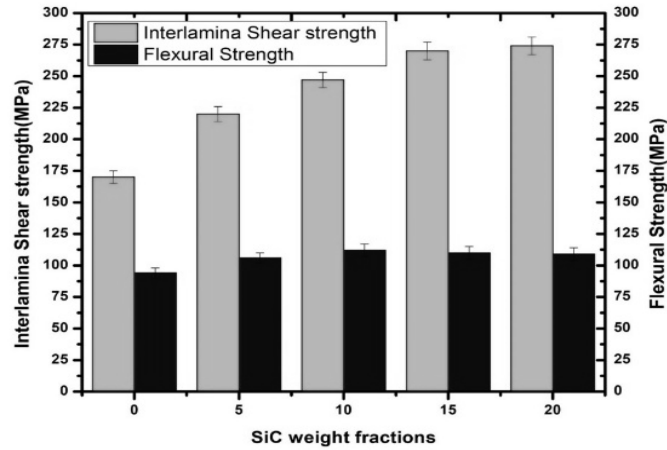


Figure 9: Flexural strength and ILSS of composites with various weight fractions of SiC/26  $\mu\text{m}/0^\circ/90^\circ$

Similarly, the interlaminar shear strength (ILSS) demonstrates an upward trend with higher SiC content. The ILSS values increase from 170 (0% SiC) to 274 (20% SiC), indicating that SiC filler of size 26  $\mu\text{m}$  enhances the composite’s interlaminar shear strength. The adherence of SiC particles to the fibers contributes to resistance to shear stress transfer. However, the flexural strength follows a different pattern. While it shows improvement with increasing SiC weight percentage, rising from 94 (0% SiC) to 112 (10% SiC), it starts to decrease beyond 10% SiC content (110 for 15% SiC and 109 for 20% SiC). This decrease in strength is due to SiC particles being stiffer and less ductile than the epoxy matrix and carbon fibers, making the composite more susceptible to brittle failure.

### Microstructural analysis

Figure 10 shows the microstructural images of fractured tensile samples of epoxy hybrid composites at different magnifications. The microcracking observed in the matrix is identified as the primary cause of failure in these composites. It is worth noting that micro-cracking can occur due to pre-existing faults within the matrix.<sup>44</sup> Upon fracture of the matrix, the activation of shear stress at the interface facilitates the transmission of loads transferring from the fibers to the surrounding material. However, the extent of debonding occurring at the interface potentially impedes crack propagation. This behaviour is the result of the effective energy-absorbing mechanisms exhibited by the fibers and the matrix.

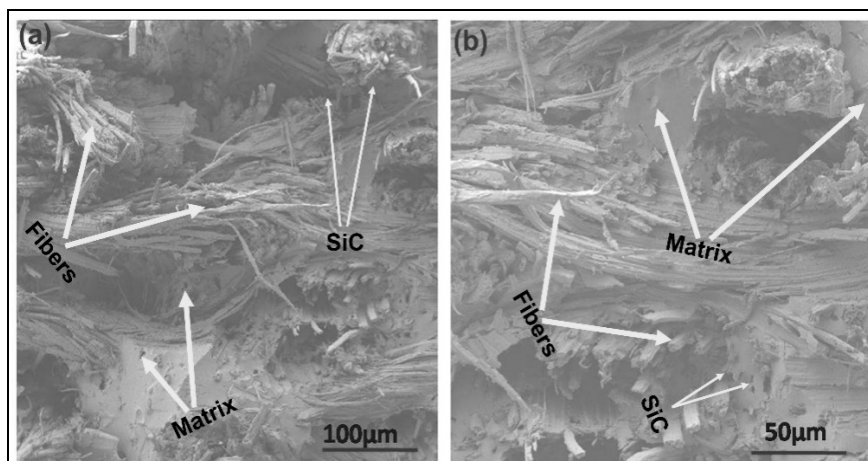


Figure 10: Microstructural images of fractured tensile samples of epoxy hybrid composites (Carbon fabric/10% SiC/26  $\mu\text{m}/0^\circ/90^\circ$ )

## CONCLUSION

The Taguchi L<sub>9</sub> design of experiments (DoE) was conducted to examine the effects of different parameters on the mechanical properties of epoxy hybrid composites through ANOVA analysis. The experimental values and ANOVA predicted results were compared and discussed. In contrast to the composites devoid of SiC, epoxy composites filled with SiC showed notable enhancements in mechanical properties. The test results support the following conclusions:

- The study demonstrated that using SiC particles with a size of 26 μm, 0°/90° fiber orientation, and SiC weight percentage ranging from 10 to 15 percent resulted in noticeable enhancements in overall mechanical performance.

- Epoxy hybrid composites exhibited a higher hardness value of 153 HV, when using the SiC particle size of 26 μm, SiC weight proportion of 20%, and fiber orientation of 0°/90°.

- The integration of fiber reinforcement significantly improved the tensile performance of the composites due to the superior mechanical properties of the fibers. The study consistently showed that a filler size of 26 μm demonstrated better performance, whereas composites with SiC additions varying from 5 to 10% had higher tensile strengths. The fiber orientation of 0°/90° provided equal stress distribution in both the warp and weft directions compared to other fiber orientations. Also, this fiber orientation resulted in the highest tensile strength due to its ability to support larger weights.

- The flexural strength of composites with carbon fibers achieved a higher value of 112 MPa when using the SiC particle size of 26 μm, SiC weight proportion of 10%, and fiber orientation of 0°/90°.

- ILSS of the prepared epoxy hybrid composites exhibited an upward trend with an increasing SiC filler content. Specifically, the ILSS reached a higher value of 274 MPa when utilizing the SiC particle size of 26 μm, SiC weight fraction of 20%, and fiber orientation of 0°/90°.

## REFERENCES

- <sup>1</sup> K. B. Nilagiri Balasubramanian and T. Ramesh, *Polym. Adv. Technol.*, **29**, 1568 (2018), <https://doi.org/10.1002/pat.4280>
- <sup>2</sup> H. Wei, H. Wang, A. Li, D. Cui, Z. Zhao *et al.*, *ChemNanoMat*, **6**, 174 (2020), <https://doi.org/10.1002/cnma.201900588>
- <sup>3</sup> T. Ramakrishnan, M. D. Mohan Gift, S. Chitradevi,

R. Jegan, P. Subha Hency Jose *et al.*, *Adv. Mater. Sci. Eng.*, (2022), <https://doi.org/10.1155/2022/1088926>

<sup>4</sup> V. Arumugaprabu, R. D. J. Johnson, M. Uthayakumar and P. Sivaranjana, "Polymer-Based Composites: Design, Manufacturing, and Applications", CRC Press, 2021, <https://doi.org/10.1201/9781003126300>

<sup>5</sup> H. Pulikkalparambil, S. M. Rangappa, S. Siengchin and J. Parameswaranpillai, *Epoxy Compos. Fabr. Charact. Appl.*, (2021), [https://doi.org/10.1007/978-981-15-8141-0\\_52-1](https://doi.org/10.1007/978-981-15-8141-0_52-1)

<sup>6</sup> S. M. Nagarjuna Reddy Paluvai and S. K. Nayak, *Polym. Plast. Technol. Eng.*, **53**, 1723 (2014), <https://doi.org/10.1080/03602559.2014.919658>

<sup>7</sup> T. K. Das, P. Ghosh and N. C. Das, *Adv. Compos. Hybrid Mater.*, **2**, 214 (2019), <https://doi.org/10.1007/s42114-018-0072-z>

<sup>8</sup> M. I. Alam, K. M. Maraz and R. A. Khan, *GSC Adv. Res. Rev.*, **10**, 20 (2022), <https://doi.org/10.30574/gscarr.2022.10.2.0036>

<sup>9</sup> S. Begum, S. Fawzia and M. S. J. Hashmi, *Adv. Mater. Process. Technol.*, **6**, 547 (2020), <https://doi.org/10.1080/2374068X.2020.1728645>

<sup>10</sup> V. Carvelli, K. Okubo and T. Fujii, *Compos. Part B Eng.*, **224**, 109225 (2021), <https://doi.org/10.1016/J.COMPOSITESB.2021.109225>

<sup>11</sup> D. Shen and Z. Wu, *Fibers Polym.*, **22**, 3501 (2021), <https://doi.org/10.1007/S12221-021-0912-2/METRICS>

<sup>12</sup> M. A. Abd El-Baky, *Fibers Polym.*, **18**, 2417 (2017), <https://doi.org/10.1007/s12221-017-7682-x>

<sup>13</sup> M. Kayaaslan, T. Coskun, O. S. Sahin, U. M. Unlu and F. Kadioglu, *Polym. Polym. Compos.*, **30**, 09673911221119669 (2022), <https://doi.org/10.1177/09673911221119669>

<sup>14</sup> N. M. Nurazzi, M. R. M. Asyraf, S. Fatimah Athiyah, S. S. Shazleen, S. A. Rafiqah *et al.*, *Polymers (Basel)*, **13** (2021), <https://doi.org/10.3390/polym13132170>

<sup>15</sup> J. Liu, H. Liu, C. Kaboglu, X. Kong, Y. Ding *et al.*, *Appl. Compos. Mater.*, **26**, 1389 (2019), <https://doi.org/10.1007/s10443-019-09786-2>

<sup>16</sup> A. Alsaadi, J. Meredith, T. Swait, J. L. Curiel-Sosa, Y. Jia *et al.*, *Compos. Part B Eng.*, **174**, 107048 (2019), <https://doi.org/https://doi.org/10.1016/j.compositesb.2019.107048>

<sup>17</sup> M. A. S. Sujon, M. A. Habib and M. Z. Abedin, *J. Mater. Res. Technol.*, **9**, 10970 (2020), <https://doi.org/https://doi.org/10.1016/j.jmrt.2020.07.079>

<sup>18</sup> N. Hashim, D. L. A. Majid, E.-S. Mahdi, R. Zahari and N. Yidris, *Compos. Struct.*, **212**, 476 (2019), <https://doi.org/https://doi.org/10.1016/j.compstruct.2019.01.036>

<sup>19</sup> B. Muralidhara, S. P. K. Babu and B. Suresha, *High Perform. Polym.*, **32**, 1061 (2020), <https://doi.org/10.1177/0954008320929396>

- <sup>20</sup> M. Alsaadi, *Mech. Compos. Mater.*, **57**, 847 (2022), <https://doi.org/10.1007/s11029-022-10004-7>
- <sup>21</sup> J. Cho, M. S. Joshi and C. T. Sun, *Compos. Sci. Technol.*, **66**, 1941 (2006), <https://doi.org/https://doi.org/10.1016/j.compscitech.2005.12.028>
- <sup>22</sup> K. Kumaresan, G. Chandramohan, M. Senthilkumar, B. Suresha and S. Indran, *Compos. Interfaces*, **18**, 509 (2011), <https://doi.org/10.1163/156855411X610241>
- <sup>23</sup> W.-H. Chen, M. Carrera Uribe, E. E. Kwon, K.-Y. A. Lin, Y.-K. Park *et al.*, *Renew. Sustain. Energ. Rev.*, **169**, 112917 (2022), <https://doi.org/https://doi.org/10.1016/j.rser.2022.112917>
- <sup>24</sup> N. S. Patel, P. L. Parihar and J. S. Makwana, *Mater. Today Proc.*, **47**, 2709 (2021), <https://doi.org/https://doi.org/10.1016/j.matpr.2021.03.005>
- <sup>25</sup> A. H. Bademlioglu, A. S. Canbolat and O. Kaynakli, *Renew. Sustain. Energ. Rev.*, **117**, 109483 (2020), <https://doi.org/https://doi.org/10.1016/j.rser.2019.109483>
- <sup>26</sup> B. E. Yuce, P. V. Nielsen and P. Wargocki, *Build. Environ.*, **225**, 109587 (2022), <https://doi.org/https://doi.org/10.1016/j.buildenv.2022.109587>
- <sup>27</sup> S. Dutta and S. Kumar Reddy Narala, *Measurement*, **169**, 108340 (2021), <https://doi.org/https://doi.org/10.1016/j.measurement.2020.108340>
- <sup>28</sup> S. Shojaei, S. S. Band, A. A. K. Farizhandi, M. Ghorogi and A. Mosavi, *Sci. Rep.*, **11**, 16054 (2021), <https://doi.org/10.1038/s41598-021-95649-5>
- <sup>29</sup> M. A. Karatas, H. Gokkaya and M. Nalbant, *Aircr. Eng. Aerosp. Technol.*, **92**, 128 (2020), <https://doi.org/10.1108/AEAT-11-2018-0282>
- <sup>30</sup> H. K. Madhusudhana, M. P. Kumar, A. Y. Patil, R. Keshavamurthy, T. M. Y. Khan *et al.*, *Polymers (Basel)*, **13** (2021), <https://doi.org/10.3390/polym13173013>
- <sup>31</sup> G. S. Balan, M. Sridharan, R. Balasundaram, A. Sasikaran, M. Sagar *et al.*, *Int. J. Polym. Sci.*, **2021**, 8587383 (2021), <https://doi.org/10.1155/2021/8587383>
- <sup>32</sup> A. Y. Chen, S. Baehr, A. Turner, Z. Zhang and G. X. Gu, *Int. J. Light. Mater. Manuf.*, **4**, 468 (2021), <https://doi.org/https://doi.org/10.1016/j.ijlmm.2021.04.001>
- <sup>33</sup> A. Vedralnam, *Compos. Part B Eng.*, **157**, 305 (2019), <https://doi.org/https://doi.org/10.1016/j.compositesb.2018.08.062>
- <sup>34</sup> T. G. Yashas Gowda, A. Vinod, P. Madhu, V. Kushvaha, M. R. Sanjay *et al.*, *Polym. Compos.*, **42**, 1891 (2021), <https://doi.org/https://doi.org/10.1002/pc.25944>
- <sup>35</sup> A. S. Rajawat, S. Singh, B. Gangil, L. Ranakoti, S. Sharma *et al.*, *Polymers (Basel)*, **14**, (2022), 602 <https://doi.org/10.3390/polym14071325>
- <sup>36</sup> L. Ranakoti, M. K. Gupta and P. K. Rakesh, *Mater. Res. Express*, **6**, 085327 (2019), <https://doi.org/10.1088/2053-1591/AB2375>
- <sup>37</sup> N. Sriraman, V. M. Sreehari, R. Jayendra Bharathi, M. K. Vinu and N. Sathiyarayanan, *Mater. Today Proc.*, **50**, 2462 (2022), <https://doi.org/https://doi.org/10.1016/j.matpr.2021.10.363>
- <sup>38</sup> M. Y. Khalid, A. Al Rashid, Z. U. Arif, N. Akram, H. Arshad *et al.*, *Crystals*, **11**, 216 (2021), <https://doi.org/10.3390/CRYST11020216>
- <sup>39</sup> M. S. Zainol Abidin, T. Herceg, E. S. Greenhalgh, M. Shaffer and A. Bismarck, *Compos. Sci. Technol.*, **170**, 85 (2019), <https://doi.org/https://doi.org/10.1016/j.compscitech.2018.11.017>
- <sup>40</sup> M. Alsaadi and A. Erklig, *Mater. Test.*, **63**, 913 (2021), <https://doi.org/10.1515/MT-2021-0020/MACHINEREADABLECITATION/RIS>
- <sup>41</sup> N. M. Z. Nik Baihaqi, A. Khalina, N. Mohd Nurazzi, H. A. Aisyah, S. M. Sapuan *et al.*, *Polimery*, **66**, 36 (2021), <https://doi.org/10.14314/POLIMERY.2021.1.5>
- <sup>42</sup> K. C. Nagaraja, S. Rajanna, G. S. Prakash, P. G. Koppad and M. Alipour, *Compos. Commun.*, **21**, 100425 (2020), <https://doi.org/https://doi.org/10.1016/j.coco.2020.100425>
- <sup>43</sup> S. Shibata, Y. Cao and I. Fukumoto, *Polym. Test.*, **24**, 1005 (2005), <https://doi.org/https://doi.org/10.1016/j.polymertesting.2005.07.012>
- <sup>44</sup> A. H. M. Ismail, F. M. AL-Oqla, M. S. Risby and S. M. Sapuan, *Carbon Lett.*, **32**, 727 (2022), <https://doi.org/10.1007/s42823-022-00323-z>